NATIONAL ADVISORY COMMITTEE FOR AERONAUTICS

TECHNICAL NOTE

No. 986

NONDESTRUCTIVE MEASUREMENT OF RESIDUAL AND ENFORCED STRESSES BY MEANS OF X-RAY DIFFRACTION

I - CORRELATED ABSTRACT OF THE LITERATURE

By George Sachs, Charles S. Smith, Jack D. Lubahn,
Gordon E. Davis, and Lynn J. Ebert
Case School of Applied Science

Washington
September 1945

NATIONAL ADVISORY COMMITTEE FOR AERONAUTICS

TECHNICAL NOTE NO. 986

NONDESTRUCTIVE MEASUREMENT OF RESIDUAL AND ENFORCED STRESSES BY MEANS OF X-RAY DIFFRACTION

I - CORRELATED ABSTRACT OF THE LITERATURE

By George Sachs, Charles S. Smith, Jack D. Lubahn, Gordon E. Davis, and Lynn J. Ebert

SUMMARY

From a study of the literature on this subject, it appears that stress measurements by means of the X-ray diffraction method have found considerable application in solving both commercial and laboratory problems.

However, an experimental and theoretical investigation of numerous factors which influence the practical execution of the X-ray method shows that the conditions in commercial structures are not conducive to accurate stress determinations.

Two selected problems that were investigated in detail will be discussed in a forthcoming report. The X-ray diffraction method revealed some fundamentally important facts regarding (a) the stress distribution in structures containing sudden section changes and subjected to elastic or plastic straining, and (b) the stress distribution within the bead of a weldment. However, the X-ray method does not appear sufficiently developed, at the present, to meet the requirements of a practical method of stress measurement, such as the following:

(a) The experimental technique should be simple.

(b) Any metal in a commercial condition should be subject to the method.

(c) The calculations should be readily performable by means of graphs, tables, or graphical methods.

(d) The results should be accurate and clearly explainable.

Thus the stress determinations by means of X-ray diffraction must be limited in the near future to research and development work, which allow a choice of the optimum metal conditions and exposure conditions for such work.

INTRODUCTION

The application of the X-ray diffraction method to the measurement of enforced and residual stresses in metal has attracted considerable interest. However, at the present, this method is not sufficiently developed to permit a commercial application.

Consequently, an attempt has been made, through the study of available information, its critical evaluation, and experimentation on variables in technique and on a few selected examples, to clarify the present situation regarding the feasibility of stress measurement.

This investigation, conducted at the Case School of Applied Science, was sponsored by and conducted with the financial assistance of the National Advisory Committee for Aeronautics.

During this work, the investigators were assisted to a considerable extent by other staff members of the Department of Metallurgical Engineering, Case School of Applied Science. Particularly appreciated is the cooperation of Prof. K. H. Donaldson, Head of the Department, Mr. F. Miller, and Mr. D. T. Doll.

HISTORY

The only destruction-free method which fundamentally permits the determination of the strain and stress states in an externally or internally strained part is the X-ray method. The first attempt of X-ray stress measurement was

made in 1925 by Lester and Aborn (reference 1), who measured the lattice parameter of a thin steel strip, subjected to tension, by means of a regular half-circular camera (fig. 1a). The strain (fig. 3) as measured by lattice parameter changes, however, could not be revealed with an accuracy sufficient for practical application. Also, the various types of cameras (fig. 1) available at that time permitted only the investigation of small articles, such as wire, sheet, or powder, but not of extended objects or structural parts.

While various methods have been successfully developed for high precision measurement of lattice parameters, using small objects, a really nondestructive method became available only in 1930 with the introduction of the flat-back reflection camera (fig. 2b) by Sachs and collaborators (references 5, 6, and 7). This camera uses the generally applied principle that a high accuracy in X-ray diffraction measurement can be obtained by the use of the reflections with the largest possible diffraction angles, that is, between 85° and 90° (fig. 1). For reflection angle of 90°, or reversely reflected beams, the experimental errors become zero. In the regular "powder" methods (fig. 1a and 1b) the line distances on one or both sides of the incident beam (fig. 4) are accurately measured. Film shrinkage and variations in the film to specimen distance are compensated by special calibration devices incorporated in the camera, or by the use of a calibration substance, such as rock salt. A further increase in accuracy and further simplification of precision measurements resulted from Van Arkel's (reference 2) suggestion of placing the film in a regular cylindrical camera with the entering (incident) beam or pinhole system as center (fig. 1c). Thus, the reflections close to 90° appear close to the center of the film (fig. 5) and their reflection angles can be determined accurately as a difference (fig. 6):

$$\frac{z\pi(180 - 2\theta)}{360} = \frac{B}{D} \text{ (in radians)}$$

where

θ angle of diffraction

$2B$ distance between two corresponding lines

D distance between film and object

Applications of other variations of this principle include a half-cylindrical camera (figs. 1d and 2a and reference 3), a conical camera (fig. 2c and reference 9), and a cylindrical camera having the direct beam as axis (fig. 2d and reference 62).

However, so far, only the flat-back reflection camera, provided with rotary and rocking movements (see fig. 12) has become popular, because of the combination of ease of handling and high precision.[1] The term "back reflection method" today usually refers to the application of this type of camera.

The first precision X-ray stress measurements were carried out by Sachs and Weerts (reference 6) with this camera, using a copper target X-ray tube. The object was a duralumin strip subjected to bending. The investigation yielded results (figs. 7 and 8) which have initiated extended research into this field. For the investigation of iron and steel, cobalt and chromium target tubes supply, according to Van Arkel and Burgers (reference 10), a more suitable radiation than a copper target, since the copper target tube causes excessive fogging of the film. Chromium radiation has been particularly recommended for heat-treated steels (reference 65).

The theory of X-ray stress measurement has been discussed by Aksenow (reference 4) in a general manner. Sachs and Weerts (reference 6) developed the relations for back reflection. They applied the relations to exposures taken perpendicular to the surface, yielding the strain in this direction or the sum of the two principal stresses in the surface. This simple procedure frequently has been found to be satisfactory for practical purposes (references 11, 12,

---

[1]R. W. G. Wyckoff, The Structure of Crystals, 2d ed., 1931, p. 164 refers to this method as follows:

"Results of still greater accuracy can be obtained by using spectra reflected through angles of nearly 180° and recorded on photographic plate instead of film. Ordinarily the purity of the material does not justify measurements of the maximum accuracy thus attainable." In the article by C. S. Barrett, X-ray Diffraction Equipment and Methods, Symposium of Radiograph and X-ray Diffraction Methods, Am. Soc. Testing Materials, 1937, pp. 193-229, 12 out of a total of 19 figures relate to the flat-back reflection camera or to results obtained by means of this camera.

14 to 17, 20, and 30). Barrett and Gensamer (reference 18) and Haskell (reference 19) suggested the determination of the total stress state from measurements of several line distances in the film. However, the experimental measurement of the complete stress state usually follows the method developed by Glocker and his collaborators (references 21, 22, 25, 26, 40, and 44). Four exposures, one in the direction perpendicular to the surface and the other three under oblique angles, are required to determine the stress state completely. The lattice parameter of the unstrained metal can be calculated also from the measurements on the strained part. If the directions of the principal stresses in the surface are known, three exposures are sufficient. Various methods suggest a further decrease in the number of exposures (references 44, 46, 47, 60, 61, and 63) by utilizing the fact that a complete reflection circle represents the strains in various directions parallel to the elements of a cone. Thus, a single oblique exposure should be sufficient for a complete stress determination; the accuracy of such a method is, however, not sufficiently high.

One of the fundamental assumptions of the X-ray stress measurement method is the absence of stress perpendicular to the surface in the extremely thin metal layer which produces the reflected beam. This assumption has been discussed in detail and studied by Kurdjumow and collaborators (references 27, 35, 36, and 37).

EQUIPMENT

Any type of equipment which produces high voltage can be used for X-ray stress measurement, the highest required voltage being approximately 40,000 volts.

Both gas (or ion) tubes and electron tubes have been used, the latter to a considerably larger extent. The air or oil-cooled electron tube requires less space and auxiliary equipment and is, therefore, more suitable than the gas tube for portable units (fig. 9). The principal problem regarding the tube is the delivery of sufficient intensity for a considerable time, ranging from 5 minutes to many hours. It appears that the rotating target tube may offer the final solution; but so far no stress measurements have been carried out with this newest and expensive type of tube.

The target metal has been discussed already. While a copper target is suitable for aluminum alloys, cobalt targets and, to a minor extent, chromium targets have been used for the investigation of iron and steel. Iron target tubes have been recommended for stress measurement on magnesium alloys (reference 55).

Portable, shock and ray proof tube stands (fig. 9) for X-ray stress measurement have been built in Germany (references 31, 41, and 47). A simple method of securing accurate rotation of the tube by a predetermined angle has been proposed by DeGraaf and Osterkamp (reference 50 and fig. 10).

The flat-back reflection camera is generally used. It has been developed from the original separate form (fig. 11) to an attachment of the tube (references 15 and 24 and figs. 9 and 12). The rotational movement around an axis perpendicular to the film (reference 4) permits the investigation of fairly large-grained metals. However, such a movement will average the stresses present in various directions. The resulting deviation can be reduced by rocking motion or a rotation (limited) to a certain angle from the desired position, according to Gisen, Glocker, and Osswald (reference 25). If an exposure is taken on iron under 45°, and the part of the reflection circle close to the metal surface is used, the following average errors (reductions of stress) in the stress determination result under the most unfavorable conditions:

Rotation (deg)	Maximum average error (percent)
±15	-0.5
±30	-1.7
±45	-3.7
±60	-6.4
±90	-13.0

Thus, rotations up to ±30° cause only an insignificant error in the final stress, and rotations up to ±60° might be used with only a slight error in stress. Full rotation is permis-

sible if the exposure is taken perpendicular to the surface. The resulting error is approximately −7 percent.

An important part of the camera is the pinhole system, which determines the intensity of the utilized X-ray beam and to a certain extent the width of the diffraction lines which must be measured. In laboratory work, the X-rays are frequently limited to a narrow cylindrical beam by means of two circular pinholes, in order to restrict the investigation to a small spot on the surface of the metal. The spot is usually between 0.020 to 0.040 inch (1/2 to 1 mm) in diameter. This restriction will not apply to most commercial objects, and it will be sufficient for many purposes to determine the average strain and stress in an area of approximately 1/4 inch in diameter.

For special purposes, the use of a beam of rectangular cross section is recommended. This rectangular cross-sectional beam is obtained by means of a single slit in connection with the line shaped focus of the tube (reference 68). However, "sharp" diffraction lines from such large reflecting areas can be obtained only by applying the well-known focusing principle (reference 24 and fig. 13) which has been utilized frequently for other types of diffraction work. The meaning of this general geometrical condition is that a beam of light originating from a point also reflects back into a sharp point if the origin, the reflecting surface, and the image are located on the surface of the same circle. The application of this principle to back reflection in the perpendicular and oblique directions is illustrated in figures 13b and 13c. In the arrangement of figure 13c, it is necessary to block off from the X-rays the side of the film marked F, and make a subsequent exposure with the film rotated 180°. This refinement has been little used, however; it is more customary to use arrangement 13b for an oblique picture and to accept the small defocusing which results. Regarding the size of the usable beam, it has been recommended that the focusing pinhole be 0.024 inch (0.6 mm) in diameter and the front pinhole 0.040 to 0.080 inch (1 to 2 mm) in diameter. However, it should be possible to use a much larger front pinhole and correspondingly to reduce the exposure time, in many cases.

The lining up of the pinhole system with a desired spot on the surface of the subject is achieved by means of some simple device, such as a sleeve on the pinhole system.

sible if the exposure is taken perpendicular to the surface. The resulting error is approximately −7 percent.

An important part of the camera is the pinhole system, which determines the intensity of the utilized X-ray beam and to a certain extent the width of the diffraction lines which must be measured. In laboratory work, the X-rays are frequently limited to a narrow cylindrical beam by means of two circular pinholes, in order to restrict the investigation to a small spot on the surface of the metal. The spot is usually between 0.020 to 0.040 inch (1/2 to 1 mm) in diameter. This restriction will not apply to most commercial objects, and it will be sufficient for many purposes to determine the average strain and stress in an area of approximately 1/4 inch in diameter.

For special purposes, the use of a beam of rectangular cross section is recommended. This rectangular cross-sectional beam is obtained by means of a single slit in connection with the line shaped focus of the tube (reference 68). However, "sharp" diffraction lines from such large reflecting areas can be obtained only by applying the well-known focusing principle (reference 24 and fig. 13) which has been utilized frequently for other types of diffraction work. The meaning of this general geometrical condition is that a beam of light originating from a point also reflects back into a sharp point if the origin, the reflecting surface, and the image are located on the surface of the same circle. The application of this principle to back reflection in the perpendicular and oblique directions is illustrated in figures 13b and 13c. In the arrangement of figure 13c, it is necessary to block off from the X-rays the side of the film marked F, and make a subsequent exposure with the film rotated 180°. This refinement has been little used, however; it is more customary to use arrangement 13b for an oblique picture and to accept the small defocusing which results. Regarding the size of the usable beam, it has been recommended that the focusing pinhole be 0.024 inch (0.6 mm) in diameter and the front pinhole 0.040 to 0.080 inch (1 to 2 mm) in diameter. However, it should be possible to use a much larger front pinhole and correspondingly to reduce the exposure time, in many cases.

The lining up of the pinhole system with a desired spot on the surface of the subject is achieved by means of some simple device, such as a sleeve on the pinhole system.

EXPERIMENTAL PROCEDURE

In order to determine a lattice parameter with a high accuracy, generally three methods are applied. First, the distances from the film to the camera and from the direct beam to the reflection lines are measured very accurately. This is done by means of calibration marks incorporated in the camera and reproduced on the film. This principle cannot be applied to the flat-back reflection camera which does not possess a definite distance between film and object. Second, the mutual position of at least two lines permits the calculation at the lattice parameter without accurate knowledge of the distances which are also distorted by film shrinkage (references 2 and 5). This method is tedious, particularly if applied to parameters which are affected by elastic strain (reference 6). The third and generally applied principle utilizes a calibration substance (references 7, 11, 12, and 14), usually silver or gold which is attached to the surface of the investigated object for the stress measurements.

The resulting X-ray film will show, in its ideal, four lines on each side of the direct beam which is in the center of the film for four full circles with the beam as center (fig. 14c). Two of these lines are the K_α-doublet of a diffraction line of the investigated metal, the other two lines represent the K_α-doublet of a diffraction line of the calibration substance.

The lines of the object, however, are frequently quite different from this ideal shape (fig. 14). There are two types of metal conditions which might seriously impair the accuracy of stress measurement (reference 25), spotty lines (fig. 14a) appear on a stationary film if an annealed metal has big crystals. Such films cannot be measured accurately. It is recommended first that 0.005 to 0.010 inch of metal be pickled off the surface in order to remove scale, oxide, and the frequently distorted (i.e., by grinding, polishing, straightening) surface layer (reference 32). In applying the calibration powder, care has to be taken to dimension the quantity so as to give both the lines of the investigated metal and those of the calibrating substance in approximately equal intensities. A suitable method of application consists of spraying some of the gold or silver powder on Scotch tape and gluing the Scotch tape to the metal surface. Rotation (fig. 7) and the focusing principle (fig. 14) will

considerably improve the appearance of the film; in many cases annealed metals can be satisfactorily subjected to X-ray stress measurements. However, if the grains are very large, the diffraction lines might be displaced and irregular, or they might consist of several streaks (references 66 and 67). This condition renders an accurate measurement impossible.

The other condition of the metal which presents difficulties on X-ray stress measurements is characterized by the merging of the K_α-doublet into a broad line with an apparently continuous intensity distribution (fig. 15). Cold work and heat treating of steels create such an appearance. However, while it is impossible to measure such a film accurately by visual means, the photometer might frequently be employed to obtain the required accuracy (reference 25). It has been claimed also that, in this respect, chromium radiation is more suitable for the investigation of heat-treated steels than cobalt radiation (reference 65). Otherwise, the accuracy of measurements has been found the same for visual and for photometric measurements.

In the visual method, the center distances of the various lines are measured by means of a simple measuring device equipped with a vernier, or "comparator" (fig. 16). In the photometric method, the intensity of the lines is measured at frequent points and recorded (fig. 17) and the distances between the maxima determined. By repeating the measuring procedure a number of times, the tolerance of the measurements can be usually brought down to ±0.05 millimeter (±0.002 in.).

However, if the lines are very diffuse, as in figure 15, the accuracy of the measurements will be considerably reduced. In order to improve this condition, the following procedure has been recommended (reference 64). The film should be taken without rotation to show the complete diffraction circles of both the investigated metal and the calibration substance. The distance between the two α_1 lines must be measured along 12 different radii and plotted against the angle which each radius makes with some zero radius (fig. 18). Through the individual points which may scatter considerably, a more accurate trend curve of the sine type can be drawn. The desired values can be taken from this curve with an accuracy of ±0.1 millimeter (±0.004 in.) even though the individual points scatter by as much as ±0.5 millimeter (±0.020 in.).

It has been claimed that the increasing width of the lines caused by cold-working can be used as a measure of the residual stress present in the metal. While this broadening of the diffraction lines might be attributed to some "microscopic" stress between and within the crystal grains, this effect cannot be correlated with the "macroscopic" stress or the residual stress which is being discussed here. Only by means of the accurate method, explained in the next section of this report, can the distribution and magnitude of the stresses be determined.

Considerable argument has arisen regarding the magnitude of the elastic constants which must be used for the stress calculation (references 38 and 58). It appears, however, that the objections to the use of the common elastic constants have not been substantiated (references 42 and 45).

FUNDAMENTALS OF STRESS MEASUREMENT

Geometrical Relations

The position of an arbitrary direction N (fig. 19) in relation to a system of axes I, II, III, can be expressed either by two of the three angles α, β, γ, which this direction includes with the three axes, or by the "longitude" Φ and the "latitude" $\gamma = \psi$, where:

$$\left.\begin{aligned} \cos\alpha &= a_1 \\ \cos\beta &= a_2 \\ \cos\gamma &= a_3 \end{aligned}\right\} \quad \text{the direction cosine} \qquad (1)$$

$$a_1^2 + a_2^2 + a_3^2 = 1 \qquad (2)$$

$$\left.\begin{aligned} \cos\Phi &= q \\ \cos\psi &= p \end{aligned}\right\} \qquad (3)$$

$$q^2 = \frac{a_1^2}{1-a_3^2}\, p^2 = a_3^2 \tag{4}$$

$$a_1^2 = q^2\,(1-p^2), \quad a_2^2 = (1-q^2)\,(1-p^2) \tag{5}$$

These and other trigonometric relations can be particularly well followed up in a stereographic projection (fig. 19b). The meaning of the stereographic projection can be understood from a comparison with the common oblique projection (fig. 19a). The principal features of the stereographic projection (or any circular projection) are the representation of directions by points and of angles by portions of great circles.

Universal Laws of Elasticity

The following universal laws of elasticity are of importance regarding the problem of X-ray stress measurements:

$$\begin{aligned} e_1 E &= s_1 - \nu s_2 - \nu s_3 \\ e_2 E &= s_2 - \nu s_3 - \nu s_1 \\ e_3 E &= s_3 - \nu s_1 - \nu s_2 \end{aligned} \tag{6}$$

$$\begin{aligned} e_x E &= s_x - \nu s_y - \nu s_z \\ e_y E &= s_y - \nu s_z - \nu s_x \\ e_z E &= s_z - \nu s_x - \nu s_y \end{aligned} \tag{7}$$

$$\begin{aligned} e_x &= e_1 \times a_1^2 + e_2 \times a_2^2 + e_3 \times a_3^2 \\ &= (1-p^2)\; e_1 \times q^2 + e_2\,(1-q^2) + e_3 \times p^2 \end{aligned} \tag{8}$$

$$s_x = (1-p^2)\; s_1 \times q^2 + s_2\,(1-q^2) + s_3 \times p^2 \tag{9}$$

Where:

s_1, s_2, s_3 = principal stresses in directions I, II, III

e_1, e_2, e_3 = principal strains in directions I, II, III

s_x, s_y, s_z = stresses in three mutually perpendicular directions X, Y, Z where X includes the angles α_x, β_x, γ_x

e_x, e_y, e_z - strains in three mutually perpendicular directions X, Y, Z where X includes the angles α_x, β_x, γ_x

ν = Poisson's ratio

Laws of Elasticity for Surface Layers

Regarding the stress and strain conditions in the layer which is accessible to the investigation with X-rays, the important assumption is made that this layer can be considered as surface and free from normal stress. This assumption has been the subject of a special investigation (reference 37) and has been found to be valid.

Thus the normal stress perpendicular to the surface is a principal stress.

Let the axis III and Z be identical and perpendicular to the surface (fig. 21) so that:

$$s_3 = s_z = 0$$

$$e_3 = e_z$$

This simplifies the relations (6) to (9) because: $\psi_x = \psi_y = 90^\circ$, $p_x = p_y = 0$, $\Phi_y = 90^\circ - \Phi_x$, $q_y^2 = 1 - q_x^2$:

$$\begin{aligned} e_1 E &= s_1 - \nu s_2 \\ e_1 E &= s_2 - \nu s_1 \\ e_3 E &= -\nu (s_1 + s_2) \end{aligned} \qquad (10)$$

$$\begin{aligned} e_x E &= s_x - \nu s_y \\ e_y E &= s_y - \nu s_x \\ e_z E &= -\nu (s_x + s_y) \end{aligned} \qquad (11)$$

$$(e_x - e_3)\,E = s_x\,(1 + \nu) \tag{12}$$

$$\left.\begin{aligned} s_x &= s_1 \times q_x^2 + s_2\,(1-q_x^2) \\ s_y &= s_1\,(1-q_x^2) + s_2 \times q_x^2 \end{aligned}\right\} \tag{13}$$

$$s_x + s_y = s_1 + s_2 \tag{14}$$

$$\begin{aligned} s_x - s_y &= (s_1 - s_2)\,(-1 + 2q_x^2) \\ &= (s_1 - s_2) \times \cos 2\Phi_x \end{aligned} \tag{15}$$

$$e_x = e_1 q_x^2 + e_2(1-q_x^2) \tag{16}$$

X-ray Measurement and Stress Components

The simplest manner for the determination of a stress state consists of determining individually a number of (normal) stress components in selected directions in the surface. It is sufficient to consider a single such direction (X) (figs. 22 and 23).

By means of X-rays strains in the following directions may be determined:

e_3 in the direction normal to the surface (III),

e' and e'' in directions (A' and A") lying in the plane III-X and being determined by the respective values ψ' and ψ'' or p' and p'', $\Phi' = \Phi'' = \Phi_x$ or $q' = q'' = q_x$.

The stress s_x can be then calculated from any two of these three values, combining first equations (8) and (16):

$$e' = (1-p'^2)\,[e_1 q_x^2 + e_2(1-q_x^2)] + e_3 \times p'^2 = (1-p'^2)(e_x - e_3) + e_3$$

$$e'' = (1-p''^2)\,(e_x - e_3) + e_3 \tag{17}$$

$$e' - e'' = (p''^2 - p'^2)\ (e_x - e_3) \tag{18}$$

Then equations (17) or (18) and (12) are combined:

$$s_x = \frac{E}{1+\nu}\ (e_x - e_3) \tag{12a}$$

$$s_x = \frac{E}{1+\nu} \times \frac{e' - e_3}{1-p'^2} = \frac{E}{1+\nu} \times \frac{e' - e_3}{\sin^2 \psi'} \tag{19}$$

$$s_x = \frac{E}{1+\nu} \times \frac{e' - e''}{p'' - p'^2} = \frac{E}{1+\nu} \times \frac{e' - e''}{\sin^2 \psi'' - \sin^2 \psi'} \tag{20}$$

Thus, equation (19) permits the calculation of the stress component s_x from two strain values in the normal and an oblique direction. This requires two different X-ray exposures (references 22 and 25).

Equation (20), which uses two oblique strain values, can be used also to determine the stress component (s_x) from a single exposure, using the two parts of the diffraction line which belong to the intersection of the plane III-X (fig. 22) with the cone of diffraction (references 44 and 60). However, this procedure is not very accurate (reference 63).

If the directions I and II of the principal stresses in the surface are known, equations (19) and (20) can be used to calculate directly the principal stresses from a normal and two oblique exposures, yielding three strains, the normal and one each in the two planes III-I and III-II.

Determination of the Principal Stresses and Their Direction

However, if the directions I and II of the principal stresses are unknown, it is necessary to determine three stress components in the surface, preferably s_x and s_y perpendicular to each other, and a third stress s'_x in

a direction X' which includes the angle δ with the direction X (fig. 24). The stress s'_y in the direction Y' perpendicular to X' is then determined by equation (14):

$$s_x + s_y = s_1 + s_2 = s'_x + s'_y \tag{14a}$$

$$s'_y = s_x + s_y - s'_x \tag{14b}$$

The difference of the principal stresses can be calculated, using equation (15):

$$s_1 - s_2 = \frac{s_x - s_y}{\cos 2\Phi_x} = \frac{s'_x - s'_y}{\cos 2\Phi'_x} \tag{22}$$

where

$$\Phi'_x = \Phi_x + \delta$$

Three of these relations for instance:

$$s_1 + s_2 = s_x + s_y \tag{14a}$$

$$s_1 - s_2 = \frac{s_x - s_y}{\cos 2\Phi_x} \tag{22a}$$

$$s_1 - s_2 = \frac{s'_x - s'_y}{\cos 2\Phi_x + 2\delta} \tag{22b}$$

may be selected and solved for the unknowns s_1, s_2, and Φ_x:

$$2s_1 = s_x \left(1 + \frac{1}{\cos 2\Phi_x}\right) + s_y \left(1 - \frac{1}{\cos 2\Phi_x}\right) \tag{23}$$

$$2s_2 = s_x\left(1 - \frac{1}{\cos 2\Phi_x}\right) + s_y\left(1 + \frac{1}{\cos 2\Phi_x}\right) \qquad (24)$$

$$\frac{s'_x - s'_y}{s_x - s_y} = \frac{\cos(2\Phi_x + 2\delta)}{\cos 2\Phi_x} \qquad (25)$$

Equation (25) may be also written:

$$\frac{s'_x - s'_y}{s_x - s_y} = \cos 2\delta - \tan 2\Phi_x \sin 2\delta \qquad (25)$$

Since $\tan \alpha = \tan \alpha \pm 180^\circ$ an ambiguity as to principal stress direction occurs. Two possible values of Φ_x result from equation (25), differing by 90°. One value is the angle between s_x and the larger of the pair s_1 and s_2 while the other Φ_x value is the angle between s_x and the smaller of the principal stresses. This situation has caused some confusion in the literature (reference 25) because of the usual convention that $s_1 > s_2$, which convention does not necessarily apply here. No difficulty occurs if one of the Φ_x values computed from equation (25) is adopted and used in equations (23) and (24) to compute s_1 and s_2. The Φ_x value used is then by definition the angle between s_1 and s_x. The s_1 computed may be either smaller or larger than s_2.

Strain and Lattice Parameter

So far strain values e have been used throughout the calculations. The definition of the strain is:

$$e = \frac{d - d_o}{d_o} \qquad (26)$$

where d is the measured lattice plane distance, and d_o the value of this plane distance in the unstrained condition.

Thus, to determine a strain exactly, the plane distance in the unstrained condition must be known.

However, the equations determining the stresses contain strains only as strain differences, such as, in equation (19): $e'_x - e_3$, which is consequently:

$$e'_x - e_3 = \frac{d'_x - d_3}{d_o} \tag{27}$$

where d'_x is a measured plane distance in an oblique direction, and d_3 the measured plane distance in the normal direction.

This equation can be replaced within the limits of accuracy by the following equation:

$$e'_x - e_3 = \frac{d'_x - d_3}{d_3}$$

This formula contains only the directly measured lattice plane distances d'_x and d_3 in the stressed condition. Thus, in practice, a stressed part may be analyzed without knowing the lattice parameter in the unstressed condition.

Regarding the cubic metals, any change of the plane distance may be considered also as a change of the lattice parameter (a):

$$d = \frac{a}{\sqrt{h^2 + k^2 + l^2}} \tag{27}$$

where h, k, l, are the Miller indices of the particular plane.

Investigations on the Effect of Stress Raisers

One important application of X-ray stress measurement is the determination of the peak stresses and stress distribution introduced by stress raisers. The effect of stress raisers can be calculated to a very limited extent only, that is, for a few simple cases such as bores. The study of photoelastic models can be applied only to flat bars. The effect of overstrain appears to introduce a considerable uncertainty, as previously mentioned.

The circumferential stress present around the transverse bore of a twisted rod has been measured by Gisen, Glocker, and Osswald (reference 25). The rod was subjected to a nominal stress (in the cylindrical section) of ±11,500 psi. The reflecting area was limited to 0.030-inch diameter by means of a celluloid plate provided with a hole. The resulting stress (fig. 26) corresponds to the laws of elasticity, the peak stress, 45,000 psi, being four times the nominal stress and slightly below the yield point of the steel (47,000 psi). No residual stress was retained after unloading, and the applied stress state had been, therefore, an elastic one.

The same type of test has been also extended to a load which would produce a peak stress of 60,000 psi if the steel remained elastic up to this value (reference 31). However, the actual stress distribution curve (fig. 27) showed a considerably lower peak stress of only approximately 35,000 psi which is below the yield point of the steel (47,000 psi). After unloading, high residual stress was retained.

The stress concentration factors for steel tension test bars provided with 70° notches having various depths and a radius of 1/16 of the rod diameter at the bottom were determined by Kraechter (reference 57 and fig. 28). [The test bar diameter has not been reported.] The peak stress increases first, and then again decreases with increasing notch depth, approaching a uniform stress distribution with a very deep notch.

While it has been reported that X-ray stress measurements are carried out in Germany on airplane assemblies, no detailed account of such work has been published as yet.

Measurement of Residual Stresses

Another important application of X-ray stress measurement is the determination of residual stress introduced by heat treating or cold working. The residual stresses can be determined by numerous methods, most of which involve a destruction of the object. For many purposes, the determination of the surface stresses only should be sufficient.

The residual stresses retained in bent steel bars (fig. 25) and bored and twisted steel rods (fig. 27) have been already discussed. Such residual stresses created by overstraining apparently can be determined with high accuracy. Residual stress up to 40,000 psi (fig. 29) have been found to be present in commerical duralumin shapes formed from tubing (reference 33). The stress distribution in the vicinity of a Brinell indentation is illustrated in figure 30. A few measurements have been also made regarding the stresses present in gun barrels subjected to the autofrettage or expanding process (reference 64).

The residual stresses present in heat-treated steels can be also determined with a fair accuracy, according to Gisen, Glocker, and Osswald (reference 25). Some divergent results which appear to disagree with the precise stress determinations by the boring method (reference 29 and figs. 31 and 32) have been explained by the introduction of additional stresses at the surface during machining. Machining operations of surfaces to be subjected to X-ray measurements must be avoided, or a layer of 0.005 to 0.010 inch thick should be pickled off the distorted surface (reference 35). This effect is probably also responsible for the varying results obtained by Kurdjumow and collaborators (references 35 and 37) regarding the residual stresses present at the surface of parts machined from a quenched steel bar.

High residual stresses were found by means of X-rays in the surface of hot-rolled steel shapes (reference 28).

A number of X-ray stress measurements have been carried out on welded steel parts (references 13, 28, 31, 33, 64, and 69). Tension stress up to 40,000 psi was found at the surface of the welded bead, while both high tension and high compression stress may be present in the parent metal near the bead.

Vibrational Stresses

The stresses present in test specimens subjected to repeated torsion have been determined by means of a synchronously rotating screen system. Tests on steel and duralumin bars provided with a transverse bore (references 41, 43, 53, 54, and 68) show that the peak stress remains unchanged up to the stress which develops a fatigue crack. After the appearance of cracks, the stress peak is reduced; residual stress is retained after unloading. A few additional tests have been made on steel bars, subjected to repeated bending and tension-compression stresses (reference 59).

Department of Metallurgical Engineering,
Case School of Applied Science,
Cleveland, Ohio, October 1942.

REFERENCES AND BIBLIOGRAPHY

1925–1929

1. Lester, H. H., and Aborn, R. H.: The Behavior under Stress of the Iron Crystals in Steel. Army Ordnance, vol. 6, 1925–1926, pp. 120–127, 200–207, 283–287, 364–369.

2. Van Arkel, A. E.: A Simple Method for Increasing the Accuracy of the Debye–Scherrer Method. Physica, vol. 6, 1926, p. 64; Zeitschr. für Kristallographie, Mineralogie und Petrographie, vol. 67, 1928, pp. 235–238.

3. Dehlinger, U.: The Widening of the Reflections on Cold–Working Metals. Zeitschr. für Kristallographie, Mineralogie und Petrographie, vol. 65, 1927, pp. 615–631.

4. Aksenow, G. J.: Measurement of Elastic Stress in a Fine–Grained Material by the Debye–Scherrer Method. Jour. Appl. Phys. (USSR), vol. 6, 1929, pp. 3–16.

1930–1933

5. Sachs, G., and Weerts, J.: The Lattice Parameters of Gold–Silver Alloys (A New Method for the X–ray Precision Measurement of Lattice Parameters). Ann. der Phys., vol. 60, 1930, pp. 481–490.

6. Sachs, G., and Weerts, J.: Elastic Measurements by Means of X–rays. Zeitschr. Phys., vol. 64, 1930, pp. 344–358; Metallurgist, vol. 8, 1932, p. 51.

7. Ageew, N., and Sachs, G.: X–ray Determination of the Solid Solubility of Copper in Silver. Zeitschr. Phys., vol. 613, 1930, pp. 293–303.

8. Caglioti, V., and Sachs, G.: The Development of Internal Stress by Stretching. Zeitschr. Phys., vol. 74, 1932, pp. 647–654.

9. Regler, F.: A New Method for Complete X–ray Examinations of the Structure of Constructional Members. Zeitschr. Phys., vol. 74, 1932, pp. 547–564.

10. Van Arkel, A. E., and Burgers, W. G.: X-rays Suitable for the Measurement of Small Variations in the Lattice Parameter of Iron. Zetischr. Metallkunde, vol. 23, 1931, pp. 149-151.

11. Wever, F., and Moeller, H.: A Method for the Measurement of Internal Stress. Archiv für das Eisenhüttenwesen, vol. 5, 1931-1932, pp. 215-218.

12. Wever, F., and Moeller, H.: The Precision Measurement of Lattice Parameters by the Back-Reflection Method. Mitteilungen Kaiser-Wilhelm Institut für Eisenforschung, Düsseldorf, vol. 15, 1933, pp. 59-69.

13. Wever, F., and Pfarr, B.: The Formation of Lattice Distortions on Cold-Working and Their Removal on Recovering and Recrystallization. Mitteilungen Kaiser-Wilhelm Institut für Eisenforschung, Düsseldorf, vol. 15, 1933, pp. 137-145.

1934

14. Wever, F.: Application of X-ray Diffraction Methods on Practical Problems. Archiv für das Eisenhüttenwesen, vol. 7, 1933-1934, pp. 527-530; Naturwissenschaften, vol. 8, 1934, p. 401.

15. Moeller, H., and Barbers, J.: X-ray Measurement of Elastic Stress. Mitteilungen Kaiser-Wilhelm Institut für Eisenforschung, Düsseldorf, vol. 16, 1924, pp. 21-31.

16. Moeller, H.: Practical Application of X-ray Methods for Measuring Elastic Stress. Archiv für das Eisenhüttenwesen, vol. 8, 1934-1935, pp. 213-217.

17. Barrett, C. S.: Internal Stresses. A. Review, Metals and Alloys, vol. 5, 1934, pp. 131-136, 154-158, 170-175, 196-198, 224-226.

18. Barrett, C. S., and Gensamer, M.: Stress Analysis and X-ray Diffraction. Phys. Rev., vol. 45, 1934, p. 563; Phys., vol. 7, 1936, pp. 1-8.

19. Haskell, R. H.: X-ray Diffraction as Applied to Determination of Stress Conditions in Gun Steel. Masters Thesis, M.I.T., 1934.

20. Glocker, R.: X-rays and Metals Research. Zeitschr. Tech. Phys., vol. 14, 1934, pp. 422-429.

1935

21. Glocker, R.: X-ray Measurement of Elastic Stress. Zeitschr. Metallkunde, vol. 27, 1935, pp. 196-198.

22. Glocker, R., and Osswald, E.: Individual Determination of the Principal Elastic Stresses by Means of X-rays (1). Zeitschr. Tech. Phys., vol. 16, 1935, pp. 237-242.

23. Moeller, H., and Barbers, J.: X-ray Investigation of the Distribution of Stress and on Overstresses in Mild Steel. Mitteilungen Kaiser-Wilhelm Institut für Eisenforschung, Düsseldorf, vol. 17, 1935, pp. 157-166; Metallurgist, 1938, p. 136.

24. Wever, F., and Rose, A.: A Focussing Camera for the Back-Reflection Method. Mitteilungen Kaiser-Wilhelm Institut für Eisenforschung, Düsseldorf, vol. 17, 1935, pp. 33-37.

1936

25. Gisen, F., Glocker, R., and Osswald, E.: Individual Determination of Elastic Stresses by Means of X-rays (II). Zeitschr. Tech. Phys., vol. 17, 1936, pp. 145-155.

26. Glocker, R.: Individual Determination of Surface Stresses by Means of X-rays. Jahrb. L.G.L., 1936, pp. 320-333.

27. Kurdjamow, G., and Scheldak, M.: The Influence of Stresses Normal to the Surface on the X-ray Measurement of Strain. Metallwirtschaft, vol. 15, 1936, pp. 907-908.

28. Wever, F., and Rose, A.: Contribution to the Problem of X-ray Measurement of Stress in Welded Structures. Mitteilungen Kaiser-Wilhelm Institut für Eisenforschung, Düsseldorf, vol. 18, 1936, pp. 31-33.

29. Wever, F., and Moeller, H.: X-ray Measurements of Stress in Quenched Steel Shafts. Mitteilungen Kaiser-Wilhelm Institut für Eisenforschung, Düsseldorf, vol. 18, 1936, pp. 27-30.

30. Wever, F.: The Present Situation Regarding the X-ray Measurement of the Sum of the Principal Stresses. Jahrb. L.G.L., 1936, pp. 313-319.

1937

31. Moeller, H., and Gisen, F.: The Reproducibility of X-ray Measurements of Elastic Stress. Mitteilungen Kaiser-Wilhelm Institut für Eisenforschung, Düsseldorf, vol. 19, 1937, pp. 57-59.

32. Moeller, H., and Roth, A.: The Cold-Working of the Metal Surface by Various Machining Conditions. Mitteilungen Kaiser-Wilhelm Institut für Eisenforschung, Düsseldorf, vol. 19, 1937, pp. 61-63.

33. Moeller, H., and Roth, A.: X-ray Measurements of Stress in Welded and Cold-Worked Specimens. Mitteilungen Kaiser-Wilhelm Institut für Eisenforschung, Düsseldorf, vol. 19, 1938, p. 136.

34. Moeller, H., and Roth, A.: Measurements of the Width of X-ray Lines. Mitteilungen Kaiser-Wilhelm Institut für Eisenforschung, Düsseldorf, vol. 19, 1937, pp. 123-126; Metallurgist, 1938, p. 136.

35. Kurdjumow, G., and Zheldak, M.: The X-ray Measurement of Stress (I) Effect of Stresses Normal to Surface on X-ray Measurements of Strain. Tech. Phys. USSR, vol. 4, 1937, pp. 515-523.

36. Romberg, W.: X-ray Measurement of Stress (II), The Determination of the Stress-Tensor. Tech. Phys. (USSR), vol. 4, 1937, pp. 524-532.

37. Kurdjumow, G., Romberg, W., and Zheldak, N.: X-ray Measurement of Stress (III). Individual X-ray Measurement of the Three Principal Stresses in the Surface Layer. Tech. Phys. (USSR), vol. 4, 1937, pp. 533-536.

38. Moeller, H., and Strunk, G.: On the Transformation of Lattice Parameters into Stresses in the X-ray Measurements of Stress. Mitteilungen Kaiser-Wilhelm Institut für Eisenforschung, Düsseldorf, vol. 19, 1937, pp. 305-315; Metallurgist, 1938, pp. 136-137.

39. Nishihara, Toshio, and Kojima, Kohei: Measurement of the Internal Stress by X-rays. Trans. Soc. Mech. Eng., Japan, vol. 3, no. 12, 1937, pp. 203-207. (Jap. with Eng. summary).

1938

40. Glocker, R.: X-ray Measurement of Elastic Press in Constructions. Archiv. Tech. Messen, (Siemens and Halske), vol. 6, 1938.

41. Glocker, R., and Kemmitz, G.: Stress Measurements During the Process of Fatigue. Zeitschr. Metallkunde, vol. 30, 1938, pp. 1-3.

42. Glocker, R., and Schaaber, O.: Mechanical and X-ray Measurements of the Torsional Modulus of Elasticity of Iron. Ergb. Tech. Röntgenkunde, vol. 6, 1938, pp. 34-92.

43. Gisen, F., and Glocker, R.: X-ray Measurement of the Changes of the Residual Stresses in Bending Fatigue Tests. Zeitschr. Metallkunde, vol. 30, 1938, pp. 297-298.

44. Glocker, R., Hess, B., and Schaaber, O.: Individual Determination of Elastic Stresses by Means of X-rays (III). Zeitschr. Tech. Phys., vol. 19, 1938, pp. 194-204.

45. Glocker, R.: The Effect of Elastic Anisotrophy on the X-ray Measurement of Stress. Zeitschr. Tech. Phys., vol. 19, 1938, pp. 289-293.

46. Moeller, H.: The Characteristics of the X-ray and Mechanical Methods of Measuring Stress. Archiv für das Eisenhüttenwesen, vol. 12, 1938-1939, pp. 27-31.

47. Wever, F.: The Fundamentals and Applications of the Measurement of Internal Stresses by Means of X-rays. Ergb. Tech. Röntgenkunde, vol. 6, 1938, pp. 9-33.

48. Bollenrath, F., and Schied, E.: X-ray Measurement of Stress in Steel Specimens Overstrained by Bending. Z.V.D.I., vol. 82, 1938, pp. 1094-1098.

49. Mesick, B. S.: Plasticity of Metals in Cold-Worked Thick Hollow Cylinders. Doctor's Thesis, M.I.T., 1938.

50. DeGraaf, J. E., and Osterkamp, W. J.: X-ray Tube for Crystal Analysis and Stress Measurements. Jour. Sci. Instr., vol. 15, 1938, pp. 293-303.

51. Stephens, R. A.: The Measurement of Residual Stresses in Welds by X-rays. Trans. Inst. Welding, vol. 1, 1938, pp. 108-116.

52. Nishihara, Toshio, and Kojima, Kohei: Possibility of Measuring the Internal Stress of Cast Iron by X-rays. Trans. Soc. Mech. Eng., Japan, vol. 4, 1938, pp. 110-112 (Jap. with Eng. summary).

1939

53. Glocker, R., Kemnitz, G., and Schall, A.: X-ray Measurements in Impact Tests. Archiv für das Eisenhüttenwesen, vol. 13, 1939-1940, pp. 89-92.

54. Kemnitz, G.: X-ray Measurement during the Process of Fatigue. Zeitschr. Tech. Phys., vol. 20, 1939, pp. 129-140.

55. Schaaber, O.: X-ray Measurement of Stress in Light Metals. Zeitschr. Tech. Phys., vol. 20, 1939, pp. 264-278.

56. Schaaber, O.: Contributions to the Theory of X-ray Measurements of Individual Stresses by Back-Reflection Photographs with a Stationary Film. Zeitschr. Tech. Phys., vol. 20, 1939, pp. 283-286. 351.

66. Brandenberger, E.: Variations of the Lattice Parameter in Crystalline Aggregates. Schweizer Archiv für Angewandte Wissenschaft und Technik, vol. 5, 1939, pp. 354–356.

1940

67. Bollenrath, F., and Osswald, E.: X-ray Stress Measurement on Unalloyed Steels beyond the Compression Yield Point. Z.V.D.I., vol. 84, 1940, pp. 539–541.

68. Schall, A.: The Behavior of Steel and Light Metals under Breaking Stresses in Alternating Torsion Tests. Zeitschr. Tech. Phys., vol. 21, 1940, pp. 1–7.

1941

69. Slack, C. M., and Ehrke, L. F.: Field Emission X-ray Tube. Jour. Appl. Phys., vol. 12, 1941, pp. 165–168.

70. Hentsch, A.: Experience Regarding the Application of X-ray Stress Measurements on Aluminum Alloys in Airplane Manufacture. Aluminium, vol, 23, 1941, pp. 27–33.

71. Norton, J. T., and Loring, B. M.: Stress Measurement in Weldments by X-rays. Monthly Rep., Welding Res. Committee, vol. 6, 1941, pp. 284–287.

1942

72. Bollenrath, F., Hauk, V., and Osswald, E.: Residual Stresses in Pure Tension Revealed by X-ray Diffraction Method. Z.V.D.I., vol. 83, no. 5, 1939, p. 129. (Abstrated by D. Rosenthal in Welding Res. Committee of the Eng. Foundation, vol. 7, no. 6, 1942, pp. 285–286.)

73. Machlett, R. R.: An Improved X-ray Tube for Diffraction Analysis. Jour. Appl. Phys., vol. 13, 1942, pp. 398–401.

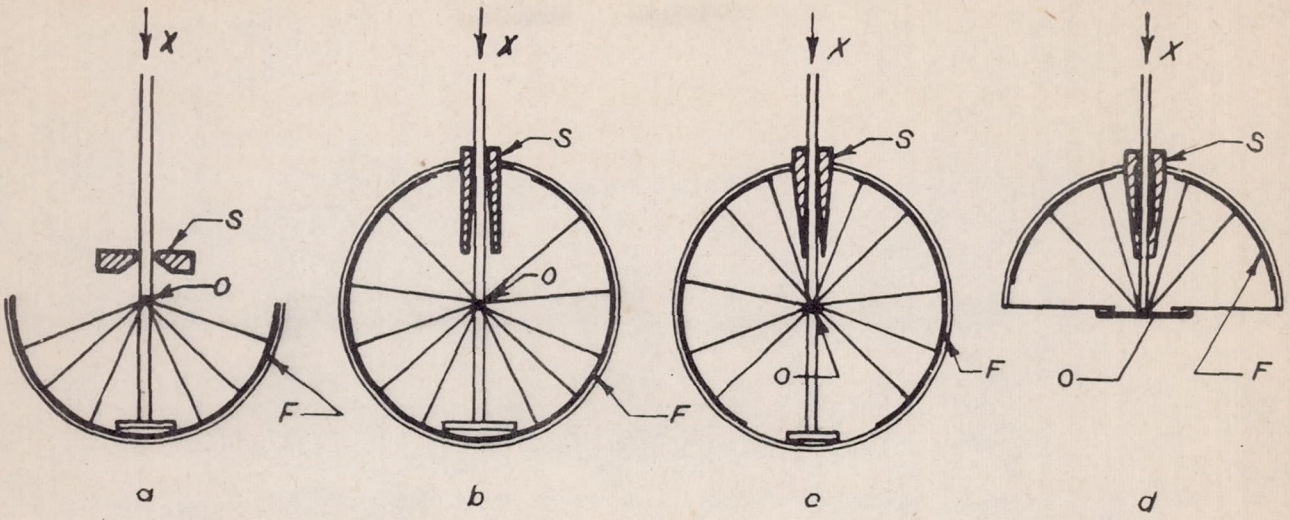

X = Direct beam
O = Object
F = Film
S = Split or pinhole system

Figure 1.- Diagrammatic representation of various X-ray powder method cameras.

a, Regular half circular camera
b, Regular circular camera
c, Back reflection circular camera
d, Back reflection half circular camera

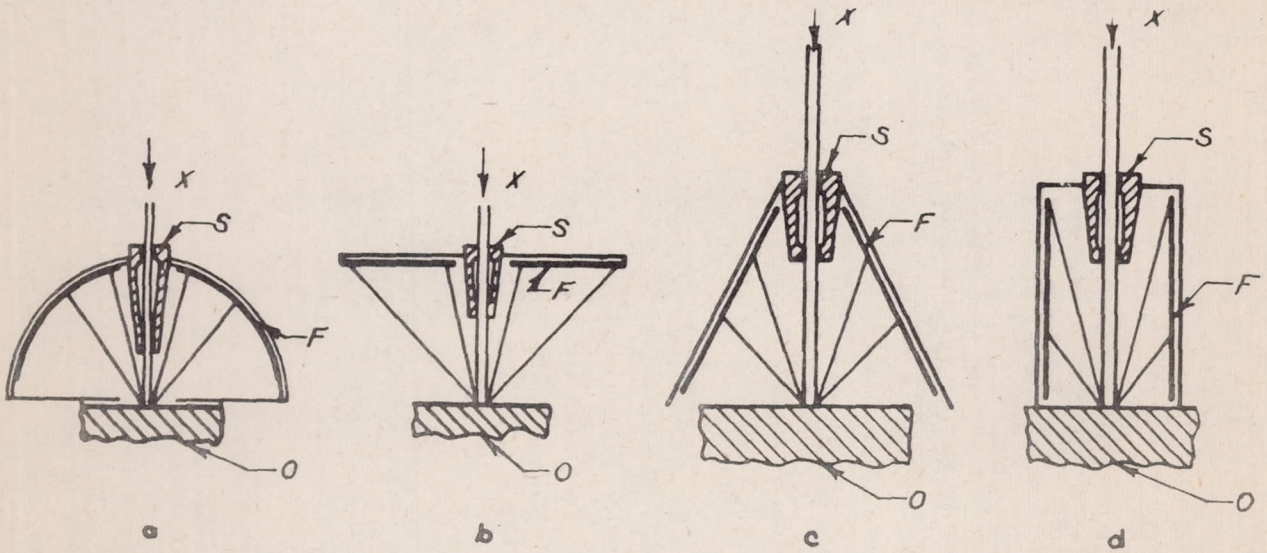

Figure 2.- Diagrammatic representation of various back reflection cameras.

a, Half circular camera
b, Flat film camera
c, Conical camera
d, Axial cylinder camera

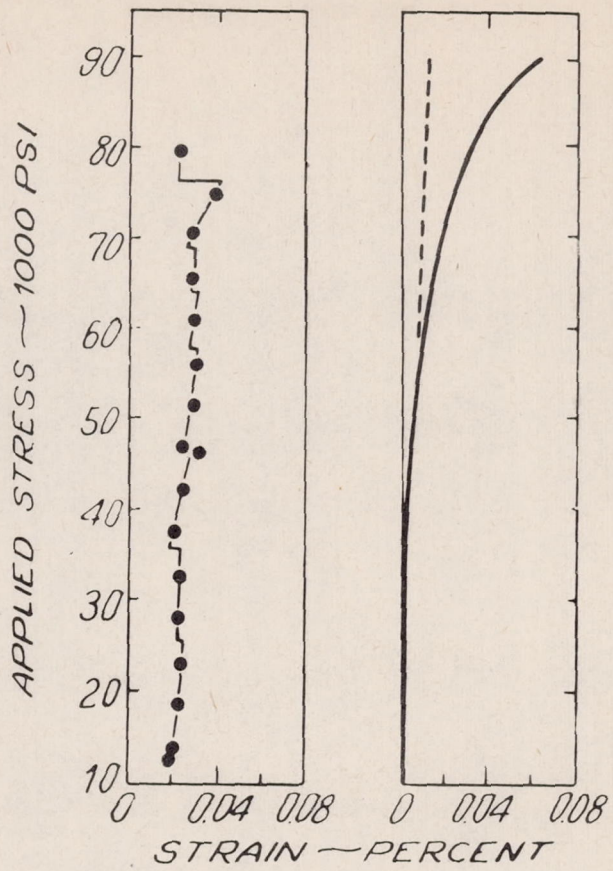

Figure 3.- Stress-strain curves of low-carbon steel as determined both by means of X-rays and mechanically, (1).

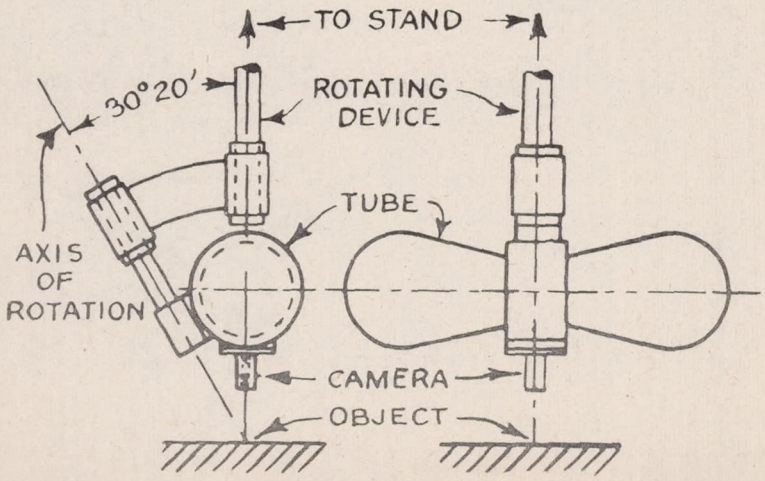

Figure 10.- Arrangement of X-ray tube for stress measurement, (50).

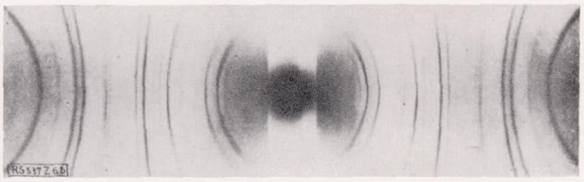

Interference lines of the K_a radiations of Cu.

Figure 4.—"Powder" X-ray diffraction pattern reflections at small Θ appear at the center of the film.

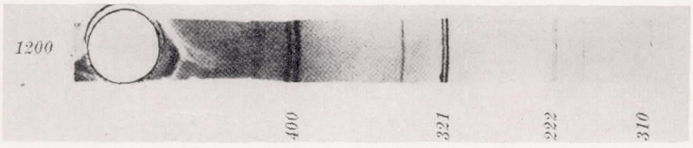

Cylindrical film perpendicular to the light beam.

Figure 5.—"Powder" pattern made with the camera loaded for back reflection measurements. Reflections at large Θ appear at the center of the film.

U. S. GOVERNMENT PRINTING OFFICE 647199

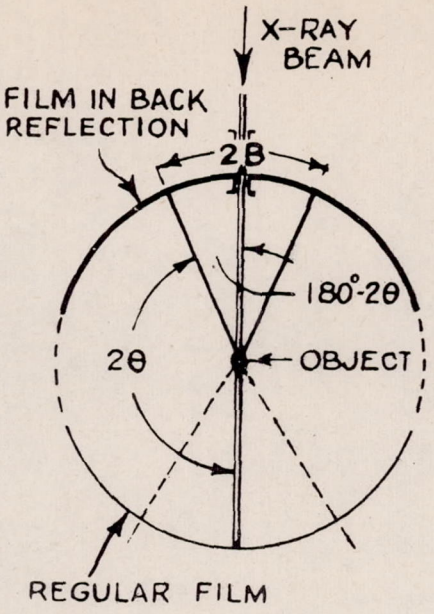

Figure 6.- Relation between line distance and diffraction angle in back reflection.

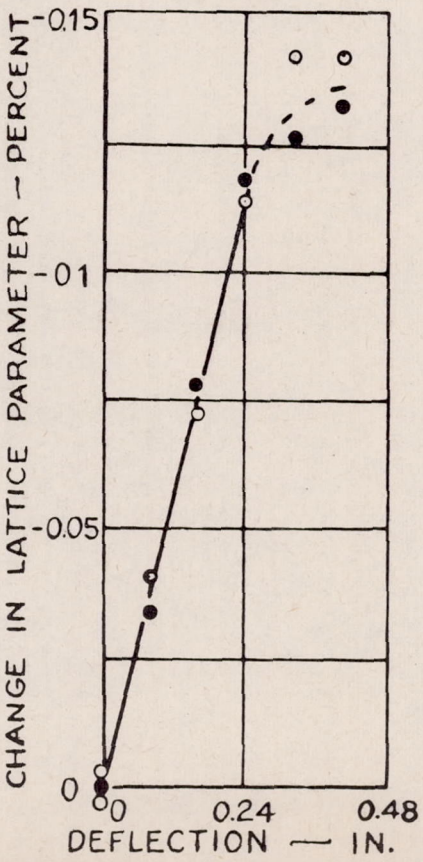

Figure 7.- Changes in lattice parameter of duralumin caused by bending, (8)

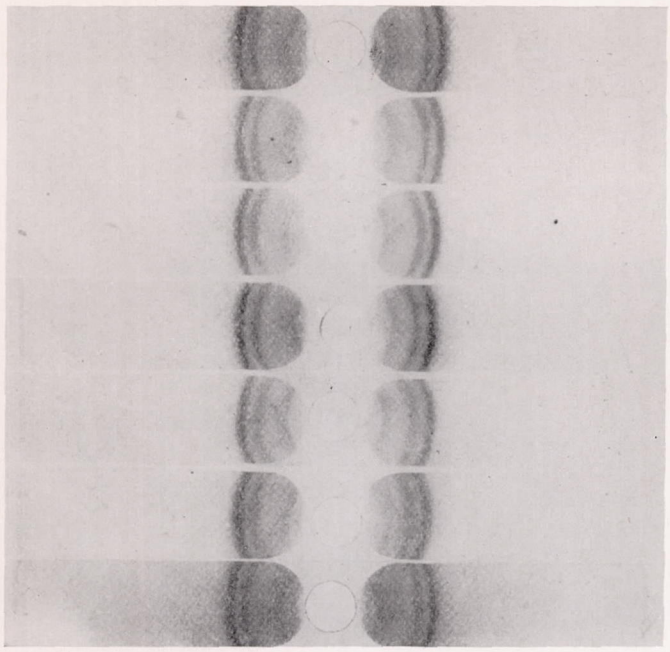

Figure 8.—Precision back reflection X-ray patterns used to measure stresses in duralumin subjected to bending.

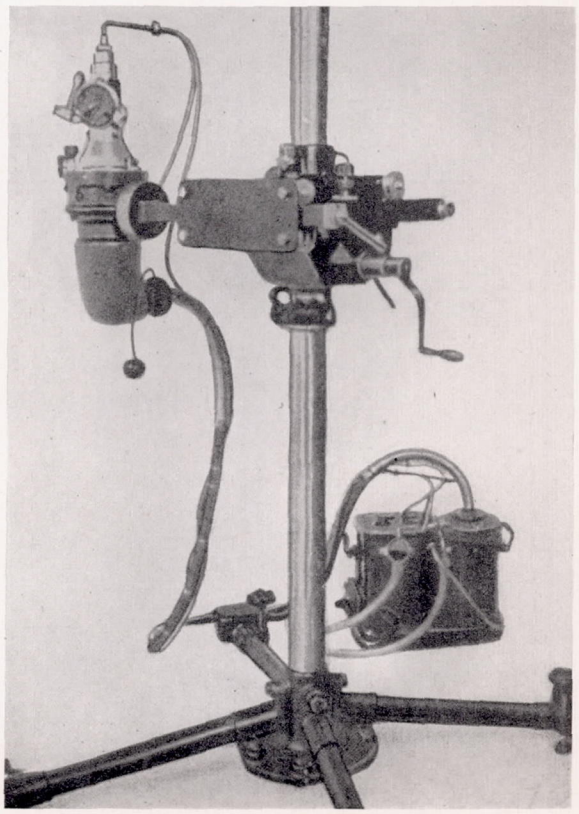

Figure 9.—Portable X-ray diffraction unit for stress measurement.

U. S. GOVERNMENT PRINTING OFFICE 647199

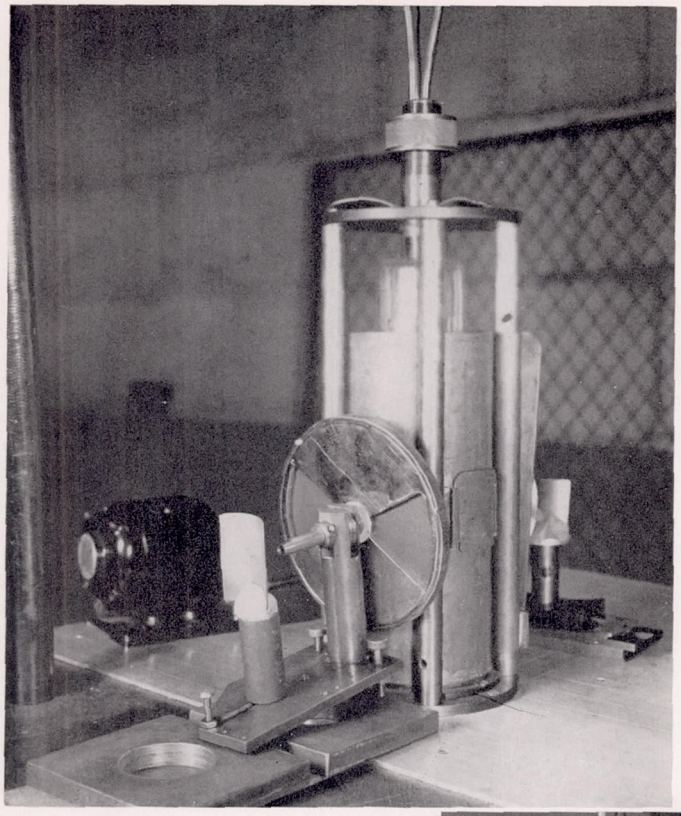

Figure 11.—Flat back reflection X-ray diffraction camera.

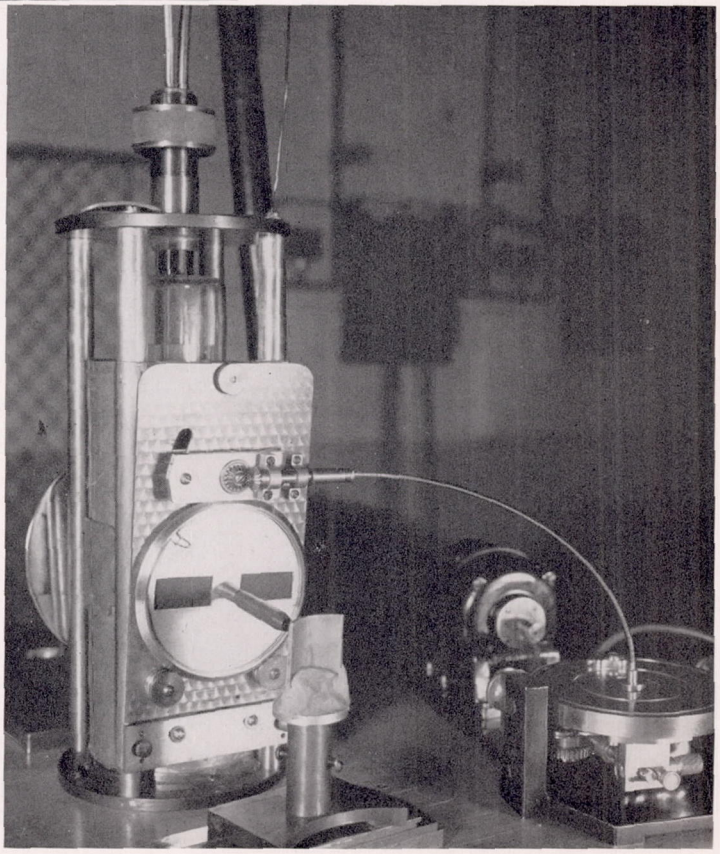

Figure 12.—Flat back reflection X-ray diffraction camera showing rocking mechanism.

U. S. GOVERNMENT PRINTING OFFICE 647199

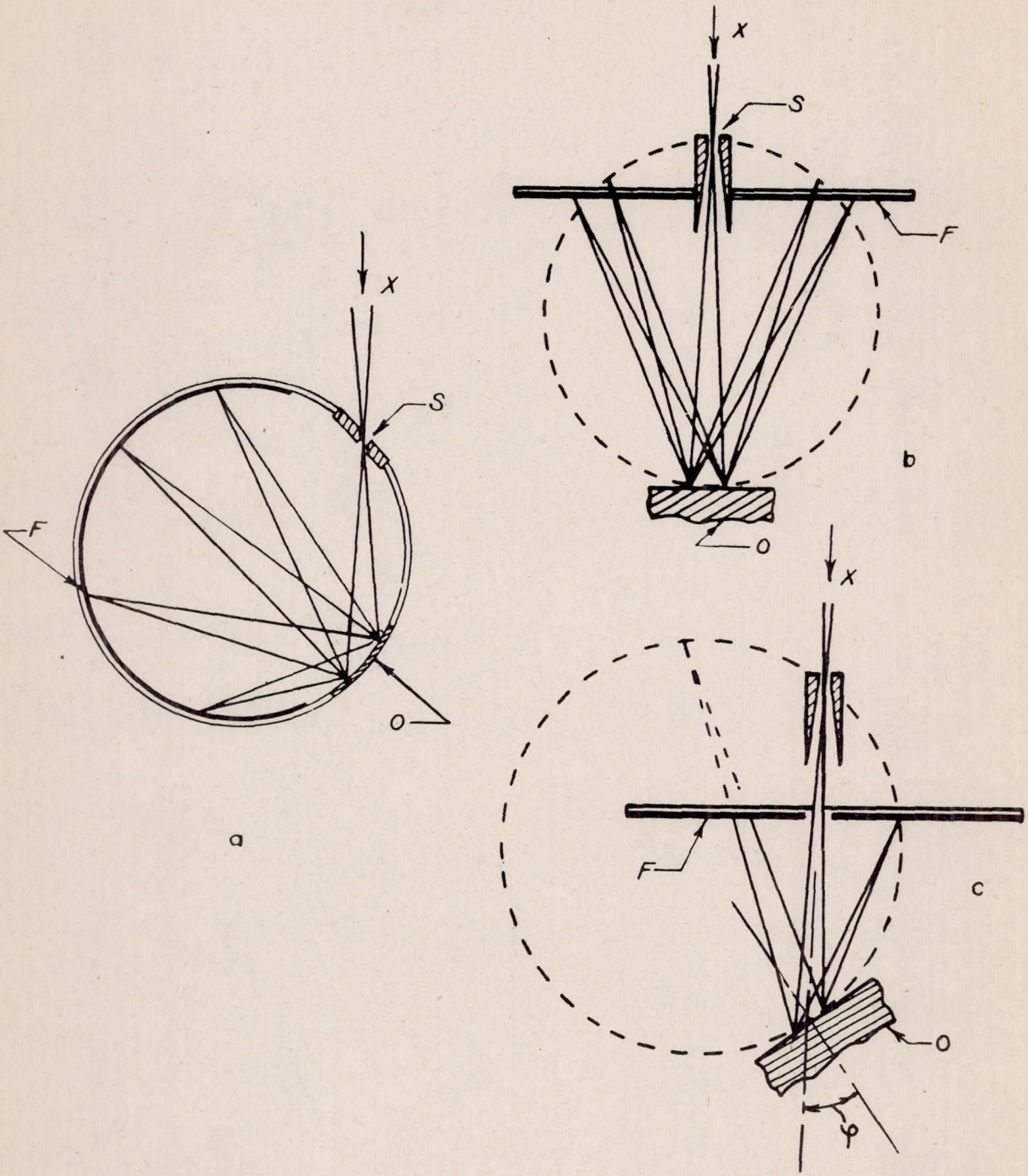

Figure 13.- Focusing conditions.

a, Circular camera
b, } Back reflection { Perpendicular surface
c, } { Oblique surface

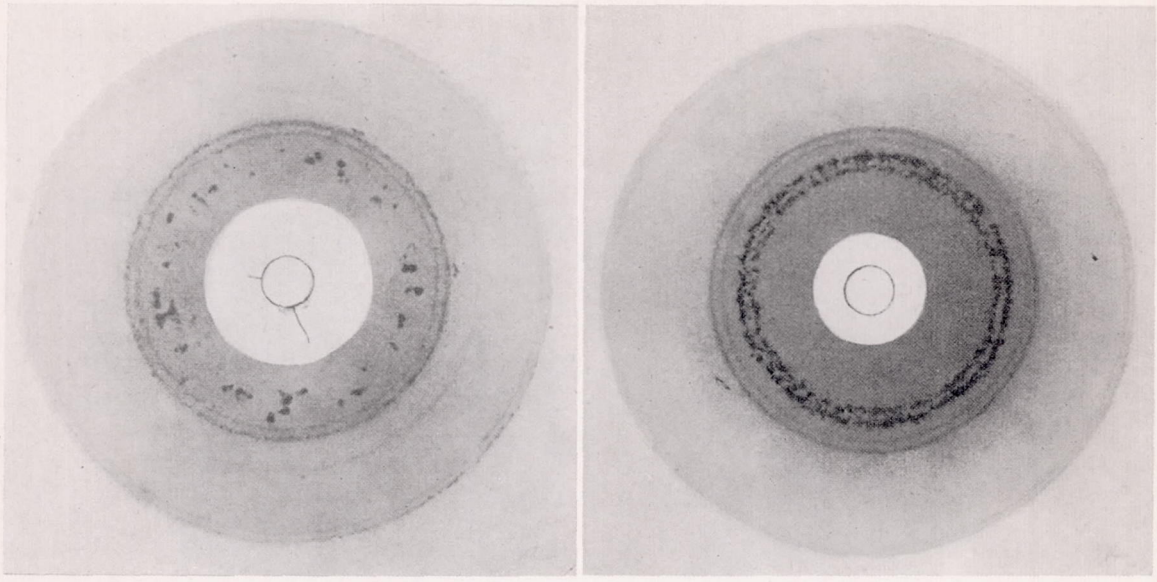

(a) A non-focusing camera with stationary film.

(b) A focusing camera with stationary film.

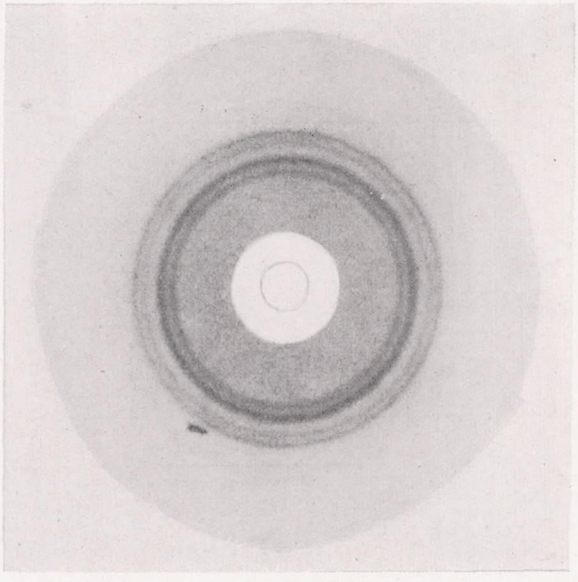

(c) A focusing camera with the film rotated.

Figure 14.—X-ray diffraction patterns.

U. S. GOVERNMENT PRINTING OFFICE 647199

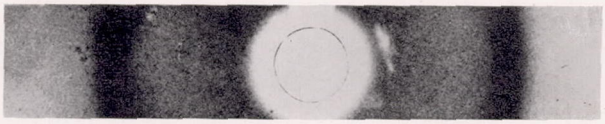

Figure 15.—Diffraction pattern showing the K_a doublet merged into a single broadline.

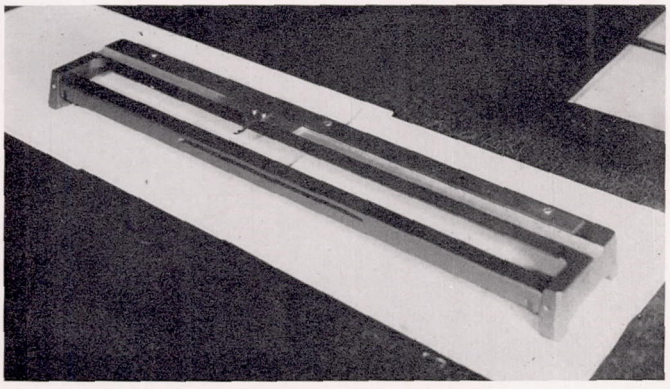

Figure 16.—Comparator for measuring diffraction patterns.

U S GOVERNMENT PRINTING OFFICE 647199

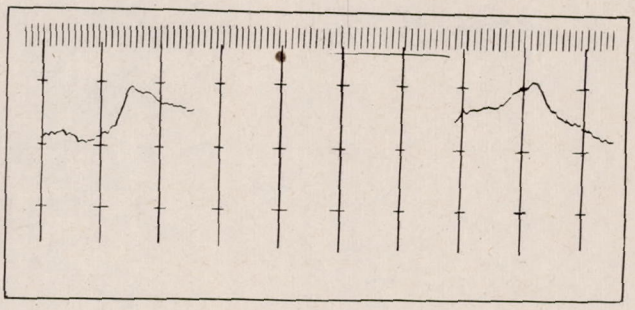

Figure 17.- Microphotometer trace of an X-ray diffraction pattern.

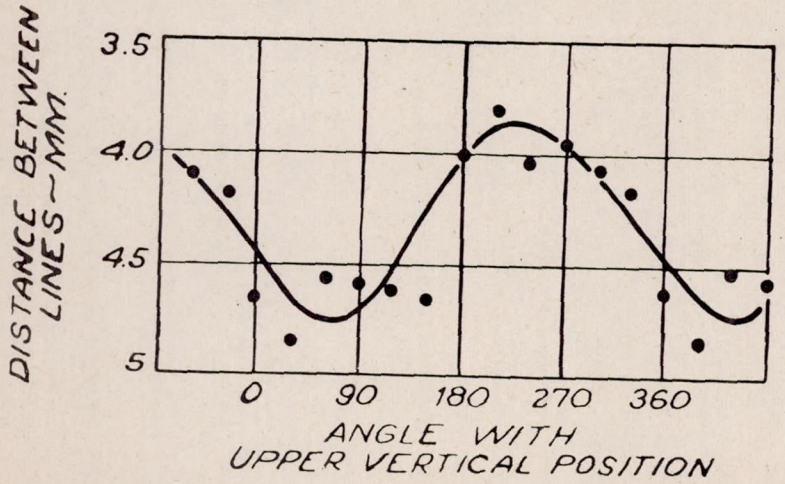

Figure 18.- Distance between steel and gold lines at various points of the diffraction circle, (64).

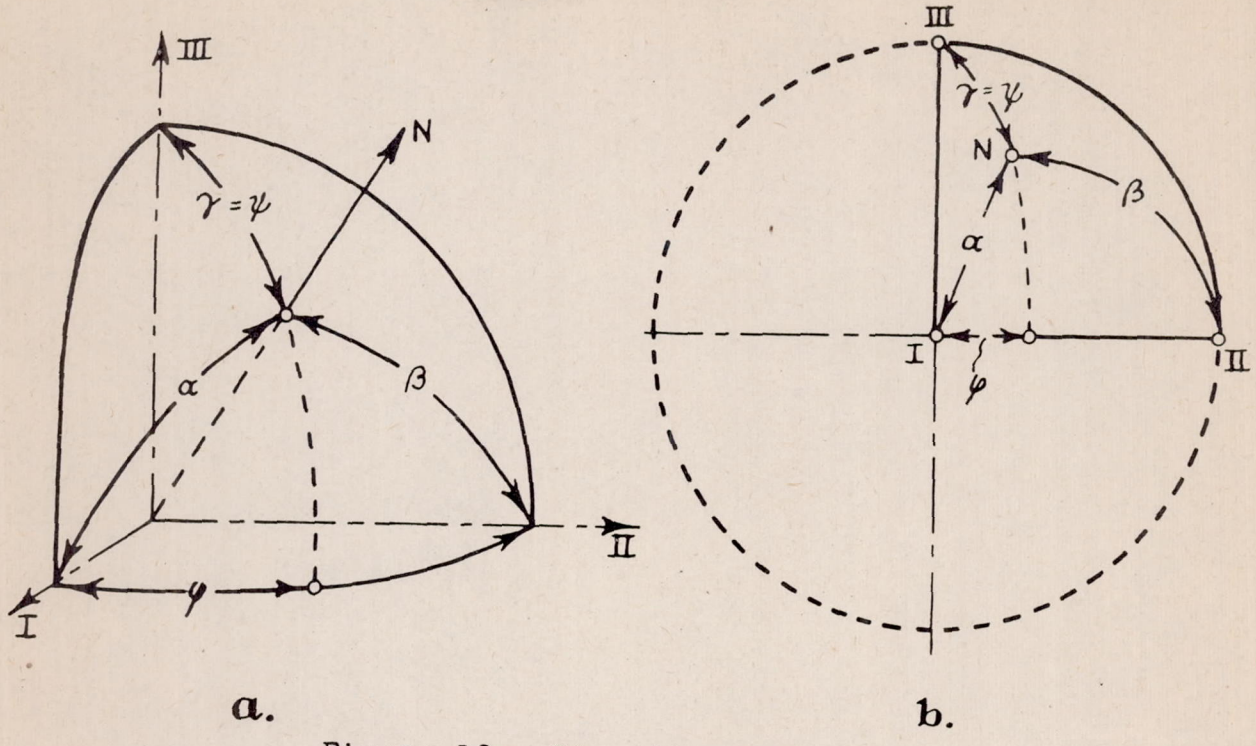

Figure 19.- Direction angles.

a, Oblique projection

b, Stereographic projection

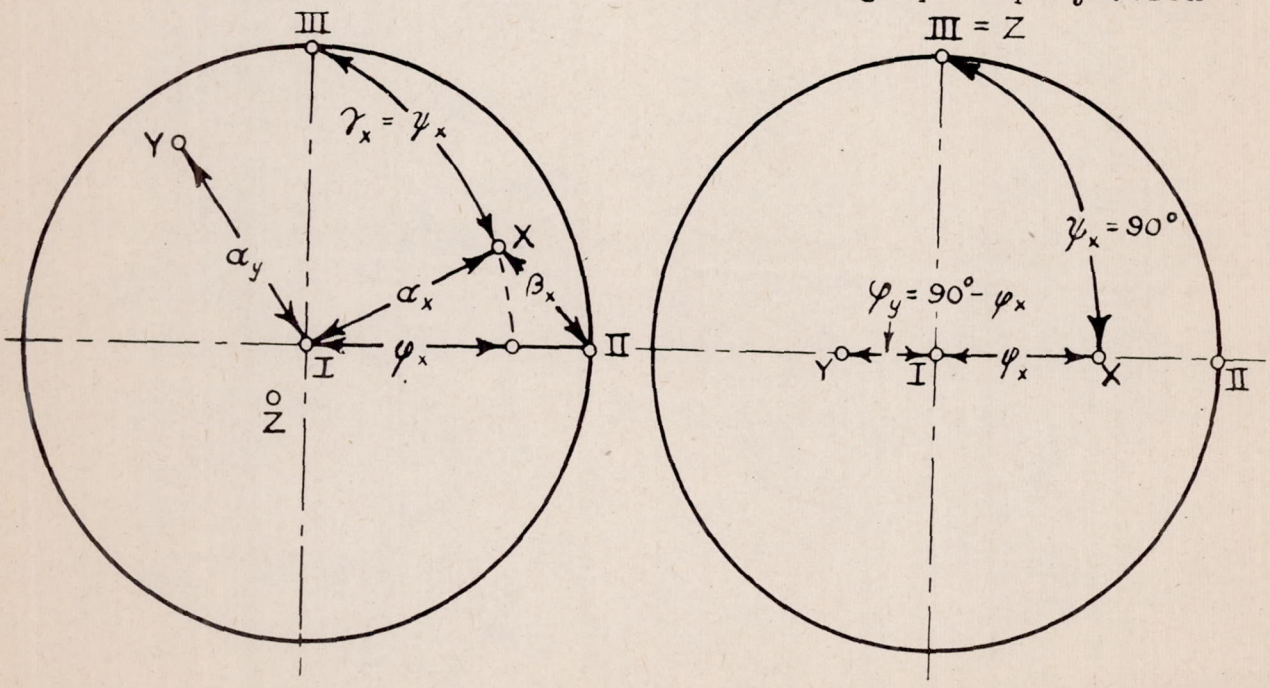

Figure 20.- Direction angles of arbitrary axes.

Figure 21.- Direction angles of axes when Z-axis is normal, to the surface.

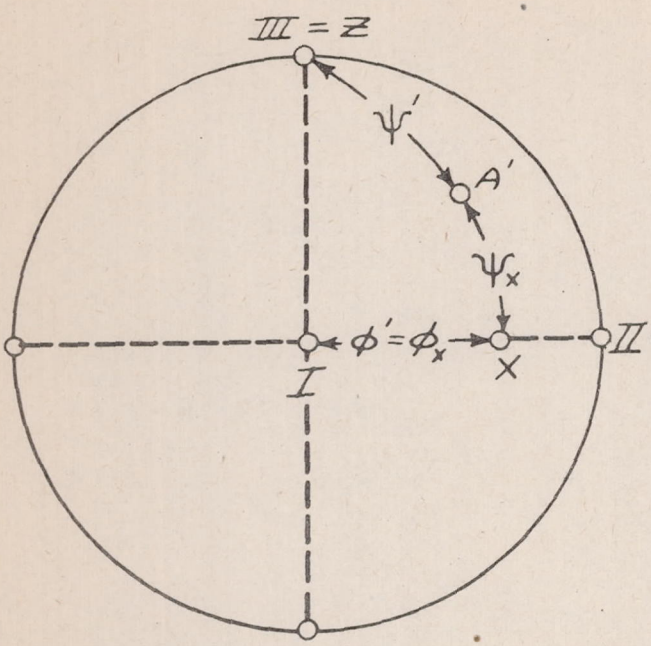

Figure 22.- Direction angles of a direction A' in the plane III - X.

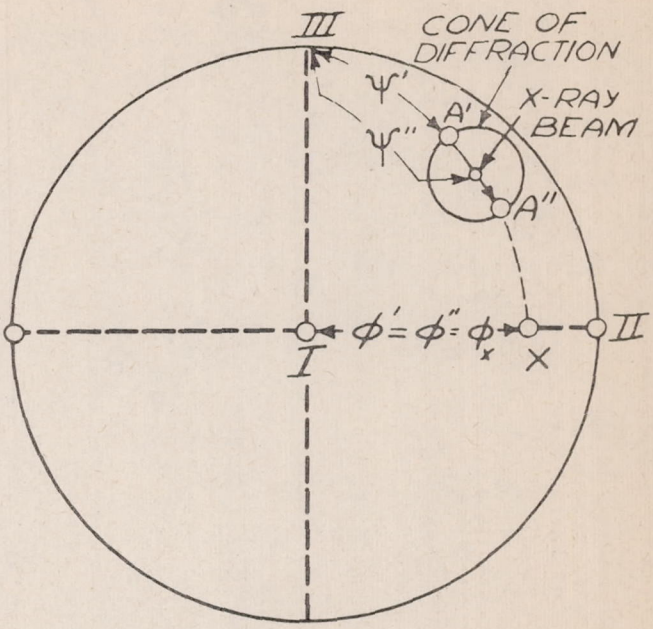

Figure 23.- Direction angles of two directions A' and A" corresponding to two opposite points of a single film.

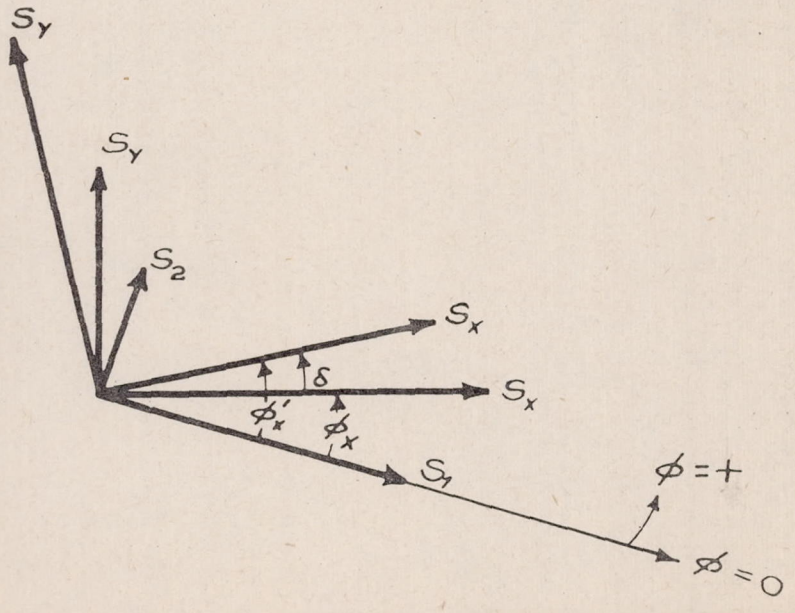

Figure 24.- Definitions of angles for the graphical solution of principal stresses.

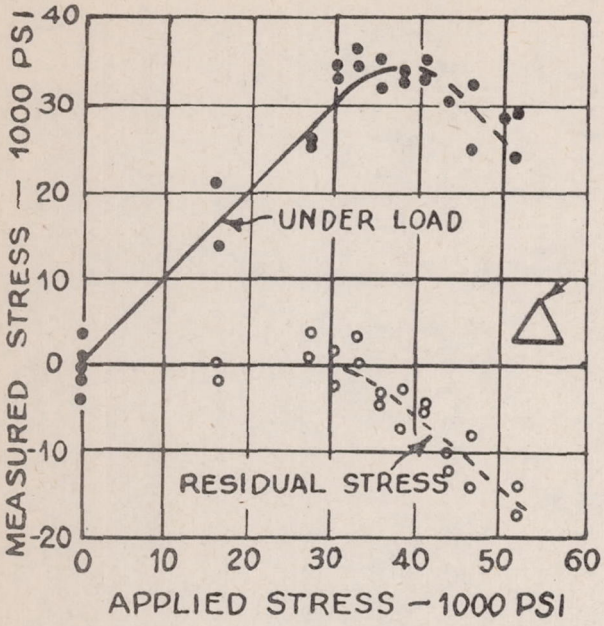

Figure 25.- Load stresses and residual stresses in a bent bar of triangular section, (48).

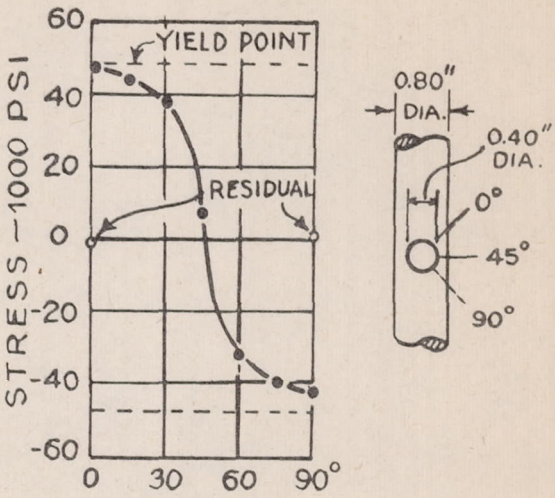

Figure 26.- Circumferential stress at edge of bore in an elastically-twisted bored steel rod, (25).

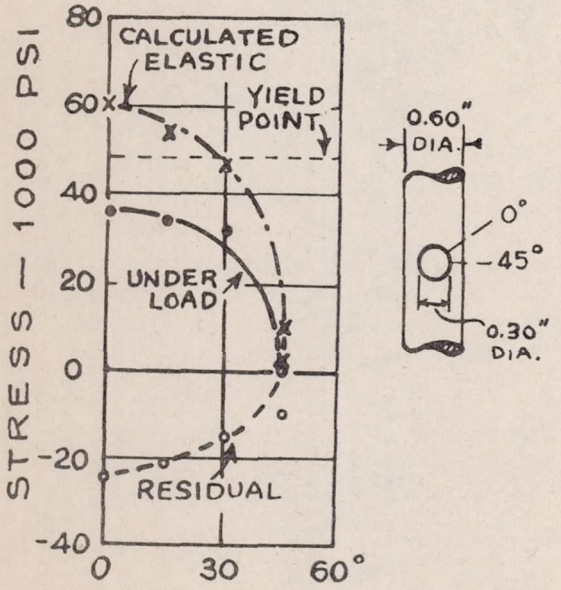

Figure 27.- Circumferential stresses at edge of bore in a plastically twisted bored steel rod, (26).

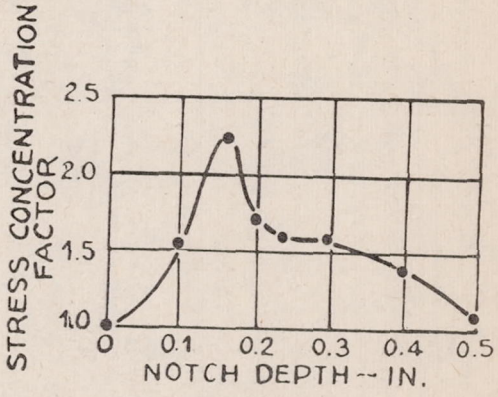

Figure 28.- Effect of notch depth on peak stress in notched tension test bars, (57).

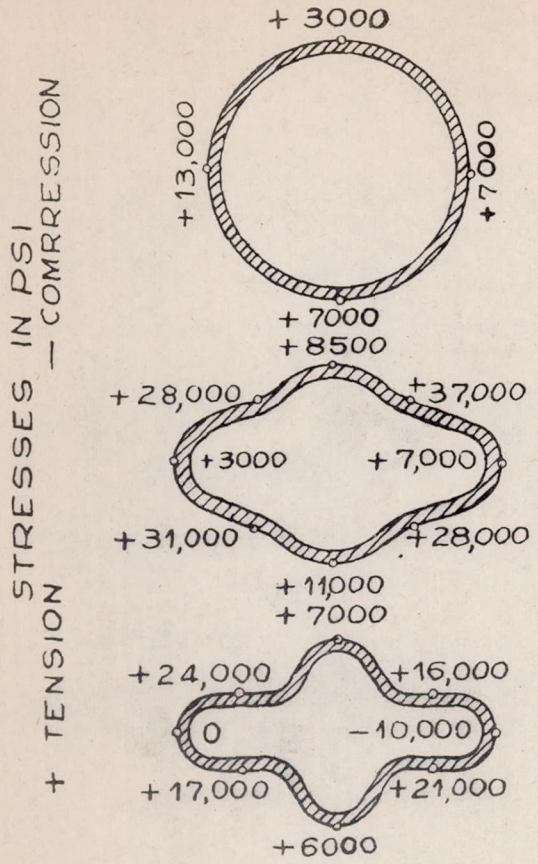

Figure 29.- Residual stress at surface of various sections of duralumin shape formed from a tube, (33).

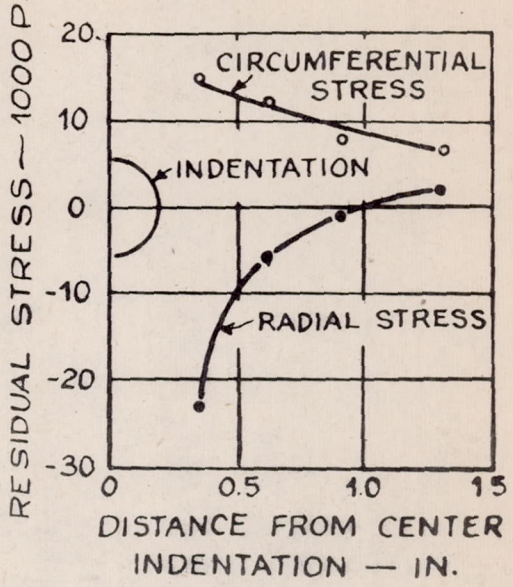

Figure 30.- Residual stresses in vicinity of ball indentation, (60).

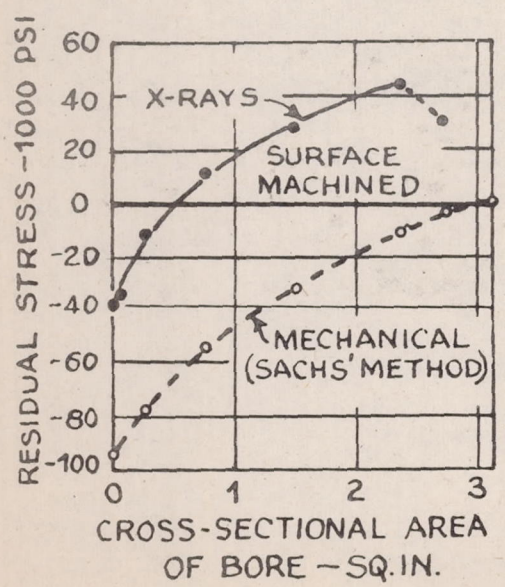

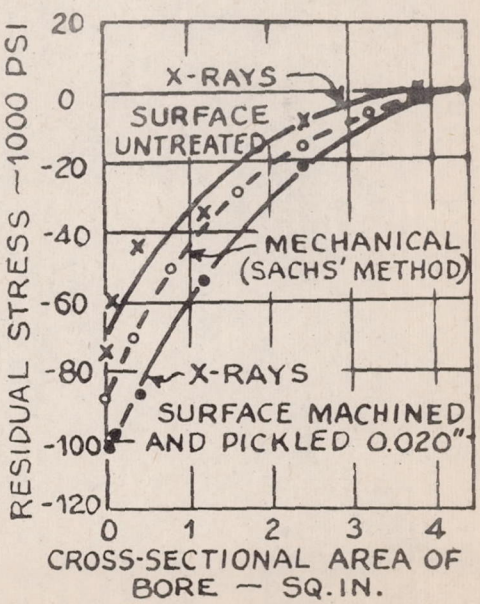

Figures 31 and 32.- Residual stress on surface of steel rods bored in steps, and effect of surface treatment on X-ray measurement, (27), (46).